Effect of constant-DI pacing on single cell pacing dynamics

P. Parthiban*,[1] S. Newell*,[a),1] and E.G. Tolkacheva[1]
1) Department of Biomedical Engineering, University of Minnesota, Minneapolis 55455, USA
** Equal Contribution*
a) Author to whom correspondence should be addressed: newel127@umn.edu

(Dated: 18 September 2020)

Cardiac alternans, beat-to-beat alternations in action potential duration (APD), is a precursor to fatal arrhythmias such as ventricular fibrillation (VF). Previous research has shown that voltage driven alternans can be suppressed by application of constant-diastolic interval (DI) pacing protocol. However, the effect of constant-DI pacing on cardiac cell dynamics and its interaction with the intracellular calcium cycle remains to be determined. Therefore, we aimed to examine the effects of constant-DI pacing on the dynamical behavior of a single cell numerical model of cardiac action potential and the influence of voltage-calcium (V-Ca) coupling on these changes. Single cell dynamics were analyzed in the vicinity of the bifurcation point using a hybrid pacing protocol, a combination of constant-basic cycle length (BCL) and constant-DI pacing. We demonstrated that in a small region beneath the bifurcation point constant-DI pacing caused the cardiac cell to remain alternans-free after switching to the constant-BCL pacing, thus introducing a region of bistability (RB). The size of the RB increases at stronger V-Ca coupling strengths and is diminished at weaker V-Ca coupling strengths. Overall, our findings demonstrate that experimental constant-DI pacing on cardiac cells with strong V-Ca strength may induce permanent changes to cardiac cell dynamics increasing the utility of constant-DI pacing.

Cardiac alternans, or the beat-to-beat alternation in action potential duration (APD), is a precursor to fatal arrhythmias such as ventricular fibrillation (VF). Previous studies have established a credible link between alternans and initiation of ventricular arrhythmias[1–4]. Hence, it is hypothesized that the elimination of alternans could prevent VF and consequent arrhythmias in the heart. Several attempts have been made over the past two decades to suppress alternans in various in-silico, in-vitro and ex-vivo models[5–12]. Pacing protocols with constant diastolic interval (DI) have suppressed voltage driven alternans. However, the effects of constant-DI pacing on cardiac cell dynamics remain unexplored.

I. INTRODUCTION

Cardiac alternans is often considered to be a precursor to tachycardia, fibrillation and other dangerous heart arrhythmias[1–4]. Thus, many strategies to eliminate alternans have been developed. Specifically, delayed feedback control was proposed to control periodic systems, such as in human patients with pacing induced period-2 atrioventricular-nodal conduction alternans[13], or small pieces of in-vitro paced bullfrog myocardium with APD alternans[14]. Delayed feedback control often applies various modifications to periodic stimulation, otherwise known as constant-BCL pacing:

$$BCL = APD_n + DI_n \tag{1}$$

where APD_n and DI_n are the APD and DI following n^{th} stimuli. When cardiac cells are paced with a constant-BCL protocol Eq. (1), a normal 1:1 response occurs at long BCL (Figure 1A), and alternans (2:2 response) occurs at shorter BCL, where APD alternates between long and short values, APD_{long} and APD_{short} (Figure 1B)[15].

Recently, we and others proposed and demonstrated the effectiveness of constant-DI pacing to eliminate alternans and establish stable 1:1 rhythms in single-cell and one-dimensional models[6,8,10]. However, the formation of alternans of cardiac action potentials under constant-DI pacing has been demonstrated in the presence of altered intracellular Ca^{2+} cycling[6]. Specifically, at rapid heart rates (low BCL) the capacity of cardiac cells to cycle intracellular Ca^{2+} is exceeded. Thus, sarcoplasmic reticulum (SR) Ca accumulates and the non-linear relationship between SR Ca load and SR Ca release becomes steep. This results in Ca transient alternans leading to a cascade of abnormal Ca^{2+}-sensitive currents that cause APD alternans[6,16,17]. Based on these findings, alternans was classified into two types: voltage (V)-driven and calcium (Ca)-driven alternans, whose mechanisms are associated with direct instabilities in transmembrane V and abnormal intracellular Ca^{2+} cycling, respectively. This is related to the fact that Ca and V are bi-directionally coupled in the cell through a variety of intracellular mechanisms. The most notable of these mechanisms is the sodium-calcium exchanger (NCX). Other mechanisms to consider include the L-type calcium current ($I_{Ca,L}$) and Ca-induced inactivation of $I_{Ca,L}$. Due to the coupling of V and Ca, the development of alternans in the Ca cycle can cause alternans in the V cycle and vice versa. It has been suggested earlier[6] that constant-DI pacing can only suppress V-driven, but not Ca-driven alternans. However, the effect of constant-DI pacing on cardiac cell dynamics has never been investigated.

In this paper, we determined the effect of constant-DI pacing on the dynamic behavior of isolated cardiac myocyte close to the bifurcation by using numerical simulations of a physiological model of cardiac action potential. We also investigated the effect of V-Ca coupling strength on the alternans formation and single cell dynamics.

II. METHODS

A. Mathematical Model

A Mahajan-Shiferaw (MS) rabbit ventricular single-cell model[18] that incorporates a well-described intracellular Ca cycle[19] at rapid heart rates was used. The sodium-calcium exchanger conductance (g_{NaCa}) was adjusted to alter the V-Ca coupling strength as shown in Table I. The slope of the SR calcium release function (u) was used to provide either V-driven (u = 9.5 s^{-1}) or Ca-driven (u = 11.3 s^{-1}) alternans, as described in[18,19].

B. Hybrid Pacing Protocol

In order to investigate whether constant-DI pacing altered the dynamical behavior of the paced cardiac cell, we implemented a *hybrid pacing protocol* consisting of four sequences:

(1) First, *constant-BCL pacing* with BCL = BCL_1 was applied to the cell (see Eq. 1 and Figure 2A, red arrows) for 5000 stimuli (blue in Figure 2C and 2D) to reach steady state. Steady state APD and DI (APD_{SS} and DI_{SS}) were calculated as the average APD and DI of the last 10 stimuli.

(2) Second, *constant-DI pacing* (see Figure 2B, red arrows) was applied for 5000 stimuli (black in Figure 2C and 2D). In order to do that, the end of each APD was measured in real time, and stimuli were applied after a predetermined DI_{const} which was calculated as:

$$DI_{const} = BCL_1 - APD_{SS}. \quad (2)$$

Steady state APD and DI (APD_{SS} and DI_{SS}) was calculated again and an equivalent BCL (BCL_{eq}) was computed as below to compare constant-BCL and constant-DI pacing:

$$BCL_{eq} = DI_{const} + APD_{SS}. \quad (3)$$

(3) Third, perturbation (δ) was applied for 100 stimuli (green in Figure 2C and 2D) at BCL_2 immediately after the constant-DI sequence:

$$BCL_2 = BCL_1 + \delta. \quad (4)$$

Figure 2C and 2D illustrate the hybrid pacing protocol without perturbation (δ = 0) and with perturbation ($\delta \neq 0$), respectively. The presence of perturbation ($\delta \neq 0$) allowed us to evaluate the reversibility of changes to the dynamical behavior of the cardiac cell caused by constant-DI pacing.

(4) Lastly, *constant-BCL pacing* at BCL = BCL_1 was applied for 4900 stimuli (red in Figure 2C and 2D) to return the system to steady state.

C. Analysis

At the end of each pacing sequence, steady state APD_{SS} was calculated at the 90% repolarization level. Bifurcation diagrams were constructed by plotting APD_{SS} as a function of BCL (during constant-BCL pacing) or BCL_{eq} (during constant-DI pacing). During alternans, APD_{long} and APD_{short} (see Figure 1B) were calculated as the respective means of odd and even beats from the last 10 steady state responses. The magnitude of alternans was computed as follows:

$$\Delta APD_a = |APD_{long} - APD_{short}| \quad (5)$$

and ΔAPD_a = 5 ms was set as the alternans threshold. The onset of alternans was defined as the smallest value of BCL (BCL_{onset}) that resulted in a 1:1 response before the transition into alternans.

TABLE I. The sodium-calcium exchanger conductance (g_{NaCa}) for each V-Ca coupling strength (taken from Ref[18]).

V-Ca Coupling Strength	Extra Strong	Strong	Normal	Weak
g_{NaCa} (uM/s)	0.75	0.80	0.84	0.88

III. RESULTS

A. Constant-DI pacing only suppresses V-driven alternans

The cardiac cell with either V-driven and Ca-driven alternans was paced using constant-BCL and constant-DI protocols, and corresponding bifurcation diagrams were then constructed. As expected, constant-BCL pacing resulted in the formation of alternans, both V-driven (Figure 3A, BCL_{onset} = 213.5 ms) and Ca-driven (Figure 3C, BCL_{onset} = 241 ms). The application of constant-DI pacing only suppressed V-driven but not Ca-driven alternans (Figure 3B and 3D), in agreement with previous studies[8,10]. Nevertheless, constant-DI pacing decreased the BCL_{onset} for Ca-driven alternans, from 241 ms to 223 ms. The model was set to the V-driven configuration for the remainder of the study because alternans was not eliminated during the Ca-driven configuration.

B. Constant-DI pacing introduces a region of bistability (RB)

In order to investigate the effect of constant-DI pacing on the dynamic responses of the cardiac cell, we applied the hybrid pacing protocol without perturbation (δ = 0, i.e. $BCL_1 \rightarrow DI_{const} \rightarrow BCL_1$). Figure 4A shows the two overlapping bifurcation diagrams: before (blue) and after (red) application of constant-DI pacing. Note that application of constant-DI pacing shifted BCL_{onset} to a lower value (see Figure 4A). Three different regions for constant-BCL pacing following constant-DI pacing were identified based on proximity to the BCL_{onset} prior to constant-DI pacing (marked in Figure 4A): (1) region 1, where $BCL_1 << BCL_{onset}$, (2) region 2, where $BCL_1 \sim BCL_{onset}$ and (3) region 3, where $BCL_1 >> BCL_{onset}$. Representative values of BCL_1 were chosen from each region

TABLE II. Dynamical responses of the cardiac cell for different regions identified in Figure 4.

Region	Constant BCL_1	Constant DI	Constant BCL_1
(1) $BCL_1 << BCL_{onset}$	2:2	1:1	2:2
(2) $BCL_1 \sim BCL_{onset}$	2:2	1:1	1:1
(3) $BCL_1 >> BCL_{onset}$	1:1	1:1	1:1

- 1) BCL_1 = 208 ms, 2) BCL_1 = 213.5 ms and 3) BCL_1 = 219 ms.

The responses of the cell to hybrid pacing are shown in Figure 4B for the three different regions. When $BCL_1 << BCL_{onset}$ the cardiac cell exhibits alternans at the end of the first constant-BCL segment. Alternans is suppressed when constant-DI pacing is applied, but reappears upon application of the second constant-BCL segment. In contrast, when $BCL_1 \sim BCL_{onset}$, the alternans at the end of the first constant-BCL segment is suppressed by applying constant-DI pacing, and subsequent constant-BCL pacing fails to re-initiate it. Such behavior suggests the presence of a region of bistability (RB), i.e. a range of BCLs in which the system can have both an alternans and 1:1 response during constant-BCL pacing. Our results also demonstrate that constant-DI pacing affects the response of the system to constant-BCL pacing. For $BCL_1 >> BCL_{onset}$ the system exhibits a stable 1:1 response independent of the pacing sequence. Therefore, our results indicate that constant-DI pacing stabilizes the dynamics of cardiac cells by eliminating alternans. These results are summarized in Table II.

C. V-Ca coupling strength affects the RB

Next, we sought to investigate the effect of V-Ca coupling strength on BCL_{onset}. The overlapping bifurcation diagrams for the down-sweep constant-BCL protocol with weak (green), normal (blue) and strong (red) V-Ca coupling (see Table 1) are shown in Figure 5. Note that increasing (decreasing) the V-Ca coupling strength decreased (increased) BCL_{onset} to 211 ms (218 ms) from the normal value of BCL_{onset} = 213.5 ms.

We then applied the hybrid pacing without perturbation (δ = 0, i.e. $BCL_1 \rightarrow DI_{const} \rightarrow BCL_1$) at varying levels of V-Ca coupling strengths (see Table I). Figure 6A and 6B show the change in the bifurcation diagrams obtained during constant-BCL pacing before (blue) and after (red) constant-DI pacing for strong and weak V-Ca coupling, respectively. Note the presence of a RB = 3 ms for strong V-Ca coupling, due to the different values of BCL_{onset} before and after constant-DI pacing. This is not the case for weak V-Ca coupling, where no RB is observed (see Figure 6B). Figure 6C compares RBs for different V-Ca coupling strengths. Note that the RB increases with increasing V-Ca coupling strength. Figure 6D demonstrates the relative shift in BCL_{onset} as a function of V-Ca coupling strength. As the V-Ca coupling strength increases, the difference between BCL_{onset} before and after application of constant-DI protocol increases, thus increasing RB. Overall, this suggests that increasing V-Ca coupling strength facilitates changes in the cell dynamics that are triggered by the application of constant-DI pacing.

D. Reversibility of bistable response is variable

Finally, we investigated if the RB triggered by constant-DI pacing can be reversed by perturbing the system. To achieve this, we applied the hybrid protocol with perturbation ($\delta \neq 0$, i.e. $BCL_1 \rightarrow DI_{const} \rightarrow BCL_2 \rightarrow BCL_1$). In Figure 7, ΔAPD (APD_{SS} – APD_{long} and APD_{SS} – APD_{short}) is plotted as a function of the value of δ for representative BCLs chosen from the RB for normal (blue) and strong V-Ca coupling (red) (BCL_1 = 213.5 ms and BCL_1 = 209 ms respectively). Note that a RB did not exist for weak V-Ca coupling, and therefore was not plotted. Changes in the cell dynamics were reversed (i.e. the cell returned to alternans) when the value of δ reached a critical value (δ_{crit}), see Table III. The inset in Figure 7 further indicates that the transition from a 1:1 response to alternans is qualitatively different for different V-Ca coupling strengths: normal V-Ca coupling resulted in a gradual increase in ΔAPD close to BCL_{onset} before a sharp increase in ΔAPD resulting in alternans while strong V-Ca coupling abruptly transitioned into alternans.

Next, the reversibility of the dynamic responses is explored for three different BCL_1 (208, 209 and 210 ms) within the RB for strong V-Ca coupling in Figure 6A. Figure 8A demonstrates three overlapping bifurcation diagrams for the BCL_1, and Figure 8B demonstrates ΔAPD as a function of δ. Moving BCL_1 closer to BCL_{onset} (211 ms) resulted in the δ_{crit} increasing from 3.6 ms (BCL = 208 ms) to 5.5 ms (BCL = 209 ms). At BCL = 210 ms, the system did not exhibit alternans (green) for any value of δ. Also, the sharpness in transition to alternans increased as BCL_1 moved closer to BCL_{onset} (comparing yellow and red traces).

IV. DISCUSSION

In this study, we first reiterated that constant-DI pacing only suppresses V-driven alternans[8,10]. We then investigated the response of the cardiac cell to constant-DI pacing in the V-driven configuration. Our main conclusions on investigating the response were: 1) Constant-DI pacing introduces a RB in the model. 2) The RB grows larger at stronger V-Ca coupling strengths and is diminished at weaker coupling strengths. That is to say, increasing V-Ca coupling facilitates changes in the cell dynamics that are triggered by constant-DI pacing. 3) The RB can be reversed by perturbing the system. The magnitude of perturbation required to reverse the RB increases as coupling strength and/or the difference between BCL_1 and BCL_{onset} increases.

A RB has not previously been observed in cardiac tissue models under constant-DI pacing. This phenomenon may be cardiac memory related because constant-DI pacing conditionally stabilizes ionic mechanisms related to cardiac memory. This new finding encourages future research into constant-DI pacing. Moreover, the RB was altered through

TABLE III. δ_{crit} required for the system to exhibit alternans after application of constant-DI pacing during strong V-Ca coupling. Respective maximum value of ΔAPD_a given for each BCL_1.

BCL_1 (ms)	δ_{crit} (ms)	max(ΔAPD_a) (ms)
208	-3.6	24.9
209	-5.5	20
210	-	0

changes in V-Ca coupling allowing for potentially further stabilization benefits.

Previous studies exhibited that coupling between V and Ca may lead to unstable voltage dynamics under preserved APD restitution[19]. In our study, we explored the possibility of the converse hypothesis where V-Ca coupling stabilizes alternating APD by creating a larger RB. In theory, under the condition of strong V-Ca coupling, the sodium-calcium exchanger is highly activated. Hence, the extrusion of Ca under rapid pacing becomes easier. This might reduce the SR calcium load and prevent instability in the calcium cycle at rapid rates. This would explain why the onset of alternans gets pushed farther with increased coupling strengths and the RB grows in size with increased V-Ca coupling. The same mechanism might enable the persistence of normal rhythm for a longer period under a strong coupling condition.

As previously mentioned, V-Ca coupling strength is modulated in the MS model by altering the conductance of the sodium-calcium exchanger (NCX). In large mammals, the NCX is a major calcium extrusion pathway and responsible for efficient balance between calcium extrusion required for relaxation and availability of calcium for SR uptake. This in turn determines the strength of the consecutive beat. Also note that the NCX is an electrogenic transporter that carries one positive charge into the cell for the extrusion of every calcium (Ca^{2+}) ion. In the case of strong coupling, where we decrease the conductance of NCX, the amplitude of the inward current decreases. Hence, the contribution of NCX during the early repolarization phase is blunted, repolarization happens sooner and the APD decreases. Please see the supplement where this relationship is clearly illustrated in Figure S3. From a global perspective, this allows the cell to relax better and have more time for local APD adaptations in order to stabilize APD alternans under rapid pacing. Similarly, during weak coupling when we increase the conductance of the NCX, the peak of the inward current increases, causing a depolarizing current while the cell is trying to repolarize. This increases APD and makes the cell prone to unstable rhythms at rapid pacing rates (see Figure S3). However, it must be noted that changing the NCX conductance significantly impacts calcium dynamics. For example, strong coupling increases the amplitude of calcium transients (see Figure S3) and a significant increase in the coupling strength could lead to calcium alternans at the cost of stabilizing the APD alternans. Hence, an intricate balance between coupling strength and pacing interval (BCL) is required to optimize the benefits of V-Ca coupling strength towards constant-DI pacing.

Several limitations of our study need to be regarded. Our analysis was conducted on numerical simulations and there is no current experimental evidence available. Hence, the results need to be validated in experimental models. However, experimental implementation of constant-DI pacing remains to be a challenge. We also studied the effects of constant-DI pacing on a single rabbit ventricular model. Our results for Figures 3 & 4 were replicated on the ten Tusscher & Panfilov ventricular epicardial single-cell model (See Fig. S1 & S2) allowing us to confirm our results are not limited to rabbit ventricular cell models. However, our results may not be present in all models as the dynamics vary across models due to differences in ionic modeling and calcium cycling. Tissue models may also have different dynamics due to cell coupling, conduction velocity restitution, and other higher-order tissue capacities. Moreover, the formulation of V-Ca coupling dynamics in the primary model studied is single-faceted and simplifies the real physiological situation of the complex interplay of calcium currents. Also, we have not analyzed the consequence of our analysis on various other calcium-sensitive ionic currents (such as Ca^{2+}-sensitive Cl^- and K^+ currents). However, the nature of action potentials under all tested coupling strengths reflected physiologic morphology validating the relevance of our findings.

Future researchers should look into Ca-alternans in the presence of varying V-Ca coupling strengths. In this study, we do not analyze Ca-alternans since we're primarily concerned about the mechanism of suppressing V-alternans. However, it has been established that the restitution of the calcium transient is independently influenced by other factors besides the DI. Hence, the possibility of Ca-alternans under cases of monotonic APD restitution and consequence of V-Ca coupling changes on these Ca-alternans need to be pursued in future studies. A detailed analysis of the nature of bifurcation under different coupling strengths needs to be conducted. Type association (smooth vs. border collision bifurcation) with coupling related changes could open new avenues to understanding alternans propagation.

We reinstate that cellular alternans has been proven to be the basis of T-wave alternans which is clinically associated with VF[4]. Further, instabilities in the calcium cycle have shown to aggravate ventricular tachycardia into fibrillation[16]. Hence, the importance of pacing strategies to eliminate alternans is paramount and the exploration of such techniques need to account for interconnected voltage and calcium dynamics. Our study proves that the intricate balance between constant-DI pacing and V-Ca coupling has the potential to permanently remodel the cardiac cell. Thus, it has a strong potential even for short term periods of pacing. Future studies in this direction will definitely provide better insight into alternans suppression.

V. CONCLUSION

In this study, we examined the effect of constant-DI pacing on cardiac cell dynamics. For this, we designed a hybrid pacing protocol with the capability to switch between constant-BCL and constant-DI pacing. We compared the state of the system before and immediately after the constant-DI pacing

sequence. We introduced short perturbations during the transition to briefly disturb the constant-DI condition and test the robustness of the induced changes. The model of the cardiac cell used for this study allows to dynamically adjust the V-Ca coupling strength and analyze the effect of the calcium cycle on changes in APD. We show that in a region close to the bifurcation point constant-DI remodels the cardiac cell. In the absence of perturbations in this region, the cell does not revert to alternans even after the constant-DI condition is removed. Increasing the V-Ca coupling strength increases the size of this region. At higher coupling strengths the changes in APD are irreversible despite large perturbations. Our study is limited to single-cell analysis and confined changes to V-Ca coupling since we alter only the sodium-calcium exchanger activity. Future research should consider investigating invasive changes to the intracellular Ca^{2+} cycle by exploring changes to other Ca transporters and expand the analysis to tissue level studies. Regardless, our results emphasize that the interaction between constant-DI pacing and V-Ca coupling provides insight into alternans propagation and elimination.

SUPPLEMENTARY MATERIAL

See the supplementary material for results on the ten Tusscher & Panfilov ventricular epicardial single-cell model[20].

ACKNOWLEDGMENTS

This study was funded by the National Science Foundation DCSD 1662250, as well as IEM UMN seed grants. The original model code for the rabbit ventricular cell was provided by Shiferaw, Y. Original model code for ten Tusscher & Panfilov ventricular epicardial single-cell model was downloaded from K. ten Tusscher's source code website.

DATA AVAILABILITY

The data that supports the findings of this study are available within the article.

REFERENCES

[1]M. L. Walker and D. S. Rosenbaum, Cardiovascular Research **57**, 599 (2003).
[2]R. L. Verrier and M. Malik, Journal of Electrocardiology **46**, 580 (2013).
[3]S. M. Narayan, Journal of the American College of Cardiology **47**, 269 (2006).
[4]J. M. Pastore, S. D. Girouard, K. R. Laurita, F. G. Akar, and D. S. Rosenbaum, Circulation **99**, 1385 (1999).
[5]U. B. Kanu, S. Iravanian, R. F. Gilmour, and D. J. Christini, IEEE Transactions on Biomedical Engineering **58**, 894 (2011).
[6]E. M. Cherry, Chaos **27**, 093902 (2017).
[7]N. F. Otani, Chaos **27**, 093935 (2017).
[8]S. Zlochiver, C. Johnson, and E. G. Tolkacheva, Chaos **27**, 093903 (2017).
[9]D. J. Christini, M. L. Riccio, A. C. Culianu, J. J. Fox, A. Karma, and R. F. Gilmour, Phys. Rev. Lett. **96**, 104101 (2006).
[10]P. N. Jordan and D. J. Christini, Journal of Cardiovascular Electrophysiology **15**, 1177 (2004).
[11]S. D. McIntyre, V. Kakade, Y. Mori, and E. G. Tolkacheva, Journal of Theoretical Biology **350**, 90 (2014).
[12]E. G. Tolkacheva, M. Nica, M. Romeo, M. Guerraty, and D. J. Gauthier, Phys. Rev. E **69**, 031904 (2004).
[13]D. J. Christini, K. M. Stein, S. M. Markowitz, S. Mittal, D. J. Slotwiner, M. A. Scheiner, S. Iwai, and B. B. Lerman, Proc. Natl. Acad. Sci. U.S.A. **98**, 5827 (2001).
[14]G. M. Hall and D. J. Gauthier, Phys. Rev. Lett. **88**, 198102 (2002).
[15]R. Wu and A. Patwardhan, Journal of Cardiovascular Electrophysiology **17**, 87 (2006).
[16]E. Chudin, J. Goldhaber, A. Garfinkel, J. Weiss, and B. Kogan, Biophysical Journal **77**, 2930 (1999).
[17]Y. Kihara and J. P. Morgan, The American Journal of Physiology **261**, H1746 (1991).
[18]A. Mahajan, Y. Shiferaw, D. Sato, A. Baher, R. Olcese, and L.-H. X. . J. N. Weiss, Biophysical Journal **94**, 392 (2008).
[19]Y. Shiferaw, M. A. Watanabe, A. Garfinkel, J. N. Weiss, and A. Karma, Biophysical Journal **85**, 3666 (2003).
[20]K. H. W. J. ten Tusscher and A. V. Panfilov, Am. J. Physiol. Heart Circ. Physiol. **291**, H1088–H1100 (2006).

Figure Caption List: Effect of constant-Di pacing on single cell pacing dynamics

1. A) Normal 1:1 response and B) alternans during periodic pacing (Eq. (1)).

2. A) Constant-BCL pacing: stimuli (red arrow) are applied at BCL_1 (see Eq. (1)). B) Constant-DI pacing: stimuli (red arrow) are applied at the end of a predetermined DI_{const} (see Eq. (2)). C) Hybrid pacing without perturbation: 5000 stimuli are applied at BCL_1 (blue) and DI_{const} (black); then 100 stimuli are applied at $BCL_2 = BCL_1$ (green), i.e. $\delta = 0$ ms in Eq. (4); finally 4900 stimuli are applied at BCL_1 (red). D) Hybrid pacing with perturbation: Similar to C), but $BCL_2 = BCL_1$ - 10 ms (green), i.e. δ = -10 ms in Eq. (4).

3. Bifurcation diagrams constructed with normal V-Ca coupling for constant-BCL (A, C) or constant-DI (B, D) pacing in the case of V-driven (A, B) and Ca-driven (C, D) alternans. Arrows indicate the onset of alternans BCL_{onset} = 213.5 ms (A), 241 ms (C) and 223 ms (D). No alternans is present in (B).

4. A) Overlap of bifurcation diagrams from hybrid pacing without perturbation: constant-BCL pacing at BCL_1 before (blue) and after (red) constant-DI pacing. Note the formation of alternans at BCL_{onset} = 213.5 ms for constant-BCL pacing before, but not after constant-DI pacing (shifted lower to 212 ms). B) Response of the cardiac cell to hybrid pacing without perturbation (i.e. $\delta = 0$) at three regions that were chosen in (A) depending on the value of BCL_1 with respect to BCL_{onset} : (1) $BCL_1 << BCL_{onset}$; (2) $BCL_1 \sim BCL_{onset}$; (3) $BCL_1 >> BCL_{onset}$.

5. The effect of V-Ca coupling strength (see Table I) on the bifurcation diagram of a cardiac cell under constant-BCL pacing. The BCL_{onset} (arrows) shift to lower values of BCL as V-Ca coupling strength increases from weak (BCL_{onset} = 218 ms) to normal (BCL_{onset} = 213.5 ms) to strong (BCL_{onset} = 211 ms).

6. Overlap of bifurcation diagrams from hybrid pacing without perturbation: constant-BCL pacing at BCL_1 before (blue) and after (red) constant-DI pacing for A) strong V-Ca coupling and B) weak V-Ca coupling. RB is indicated by dashed box in A. C) RB as a function of different V-Ca coupling strengths. D) The shift of BCL_{onset} before (blue) and after (red) constant-DI pacing for varying V-Ca coupling strengths.

7. ΔAPD as a function of δ when the hybrid pacing protocol with perturbation was applied for the case of strong (red) and normal (blue) V-Ca coupling. The inset shows the region of transition from 1:1 into alternans for the cardiac cell with normal V-Ca coupling.

8. A) Fig. 6A with three BCL_1 within the RB (Table III) clearly labeled. B) The value of alternans ΔAPD as a function of δ during the hybrid pacing protocol with perturbation for each BCL_1 listed in Table III.

Chaos

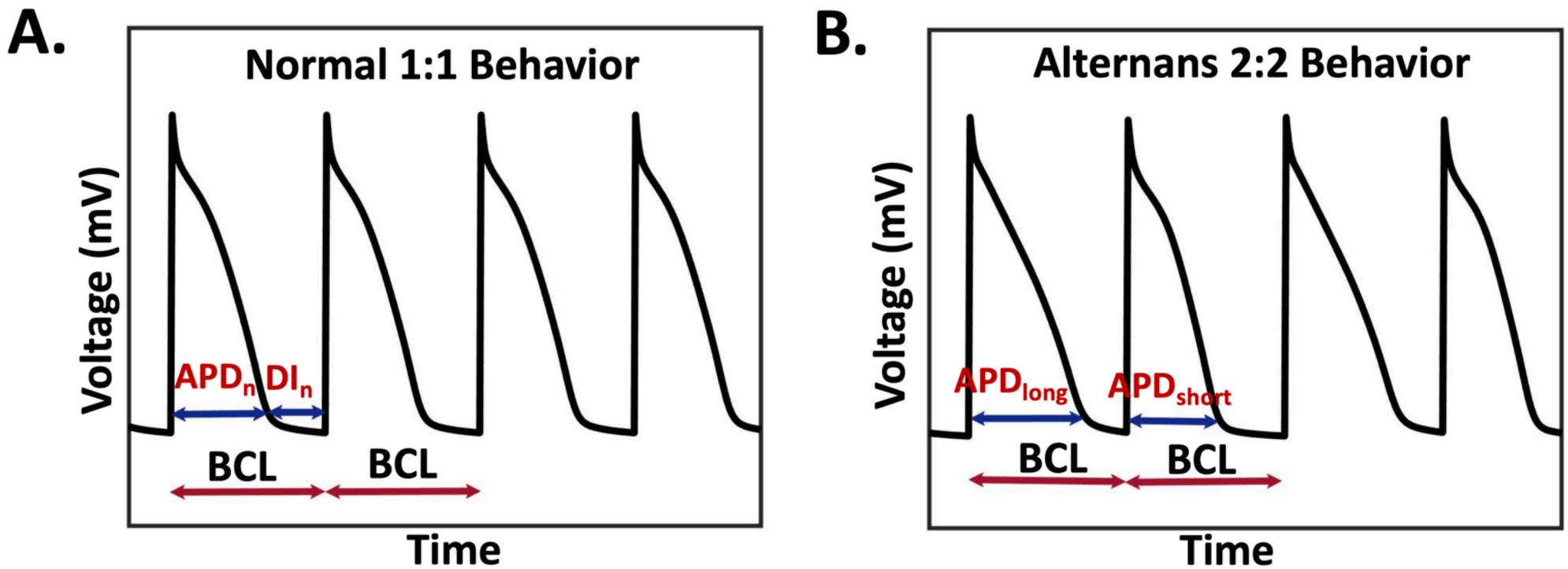

Figure 1: A) Normal 1:1 response and B) alternans during periodic pacing (Eq. (1))

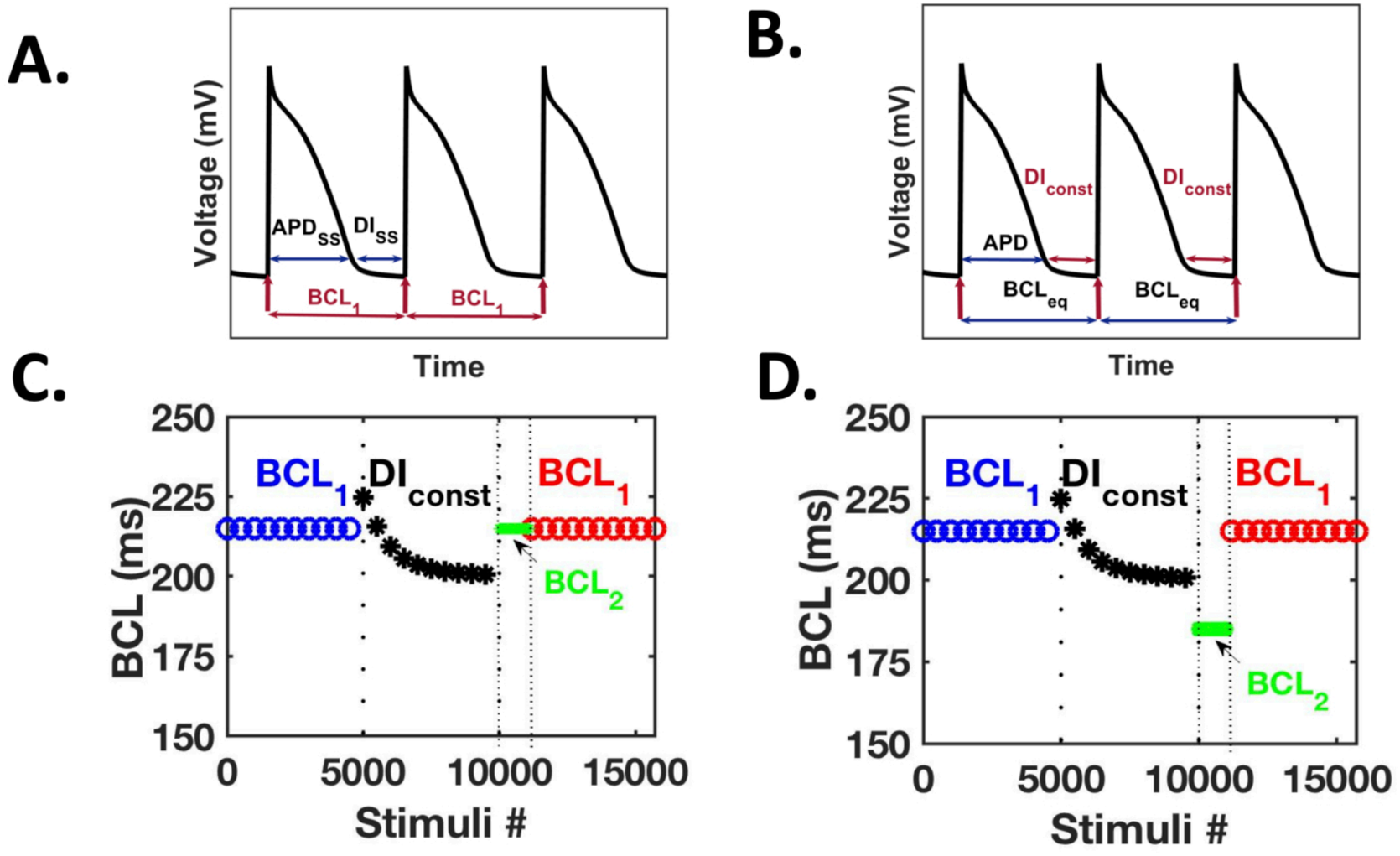

Figure 2: A) Constant-BCL pacing: stimuli (red arrow) are applied at a predetermined BCL_1 (see Eq. (1)). B) Constant-DI pacing: stimuli (red arrow) are applied at the end of predetermined DI_{const} (see Eq. (2)). C) Hybrid pacing without perturbation: 5000 stimuli are applied at BCL_1 (blue) and DI_{const} (black); then 100 stimuli are applied at $BCL_2 = BCL_1$ (green), i.e. $\delta = 0$ ms in Eq. (4); finally 4900 stimuli are applied at BCL_1 (red). D) Similar to C), but $BCL_2 = BCL_1 - 10$ ms (green), i.e. $\delta = -10$ ms in Eq. (4).

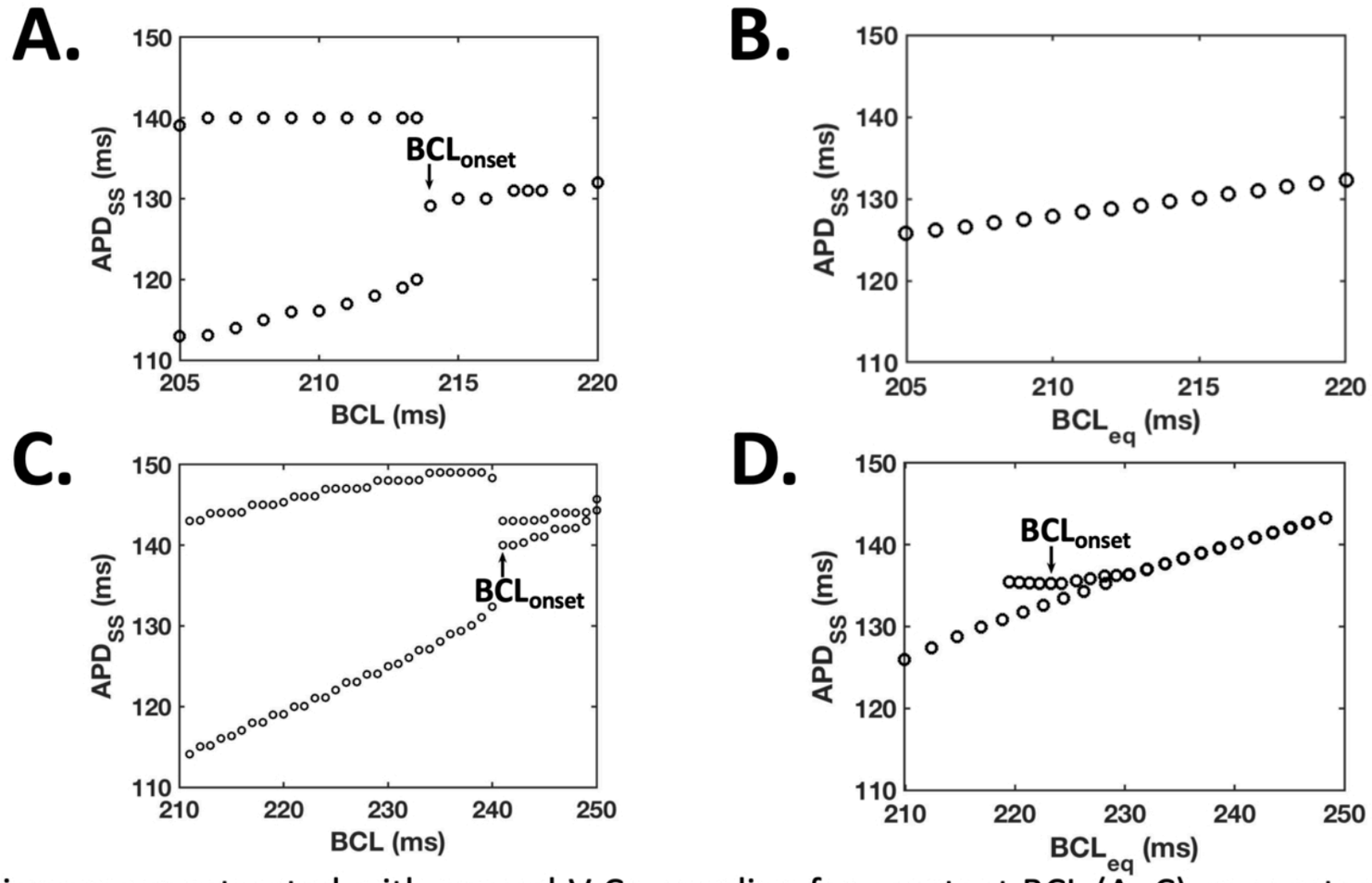

Figure 3: Bifurcation diagrams constructed with normal V-Ca coupling for constant-BCL (A, C) or constant-DI (B, D) pacing in the case of V-driven (A, B) and Ca-driven (C, D) alternan configurations. Arrows indicate the onset of alternans BCL_{onset} = 213.5 ms (A), 241 ms (C) and 223 ms (D). No alternans is present in (B).

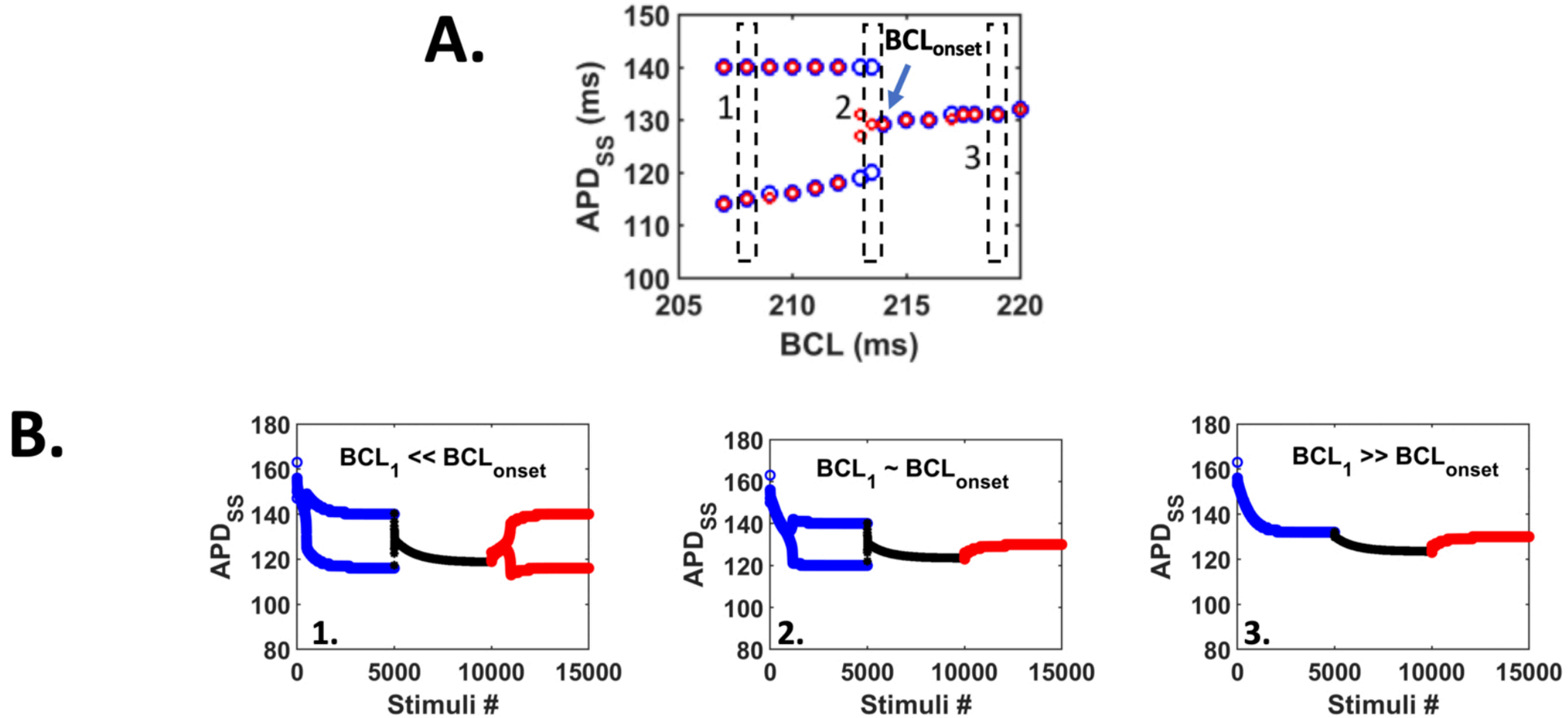

Figure 4: A) Overlap of bifurcation diagrams from hybrid pacing: constant-BCL pacing at BCL_1 before (blue) and after (red) constant-DI pacing. Note the formation of alternans at BCL_{onset} = 213.5 ms for constant-BCL pacing before (marked in A), but not after constant-DI pacing (shifted lower to 212 ms). B) Responses of the cardiac cell to hybrid pacing at three regions that were chosen in (A) depending on the value of BCL_1 with respect to BCL_{onset} : (1) $BCL_1 << BCL_{onset}$; (2) $BCL_1 \sim BCL_{onset}$; (3) $BCL_1 >> BCL_{onset}$.

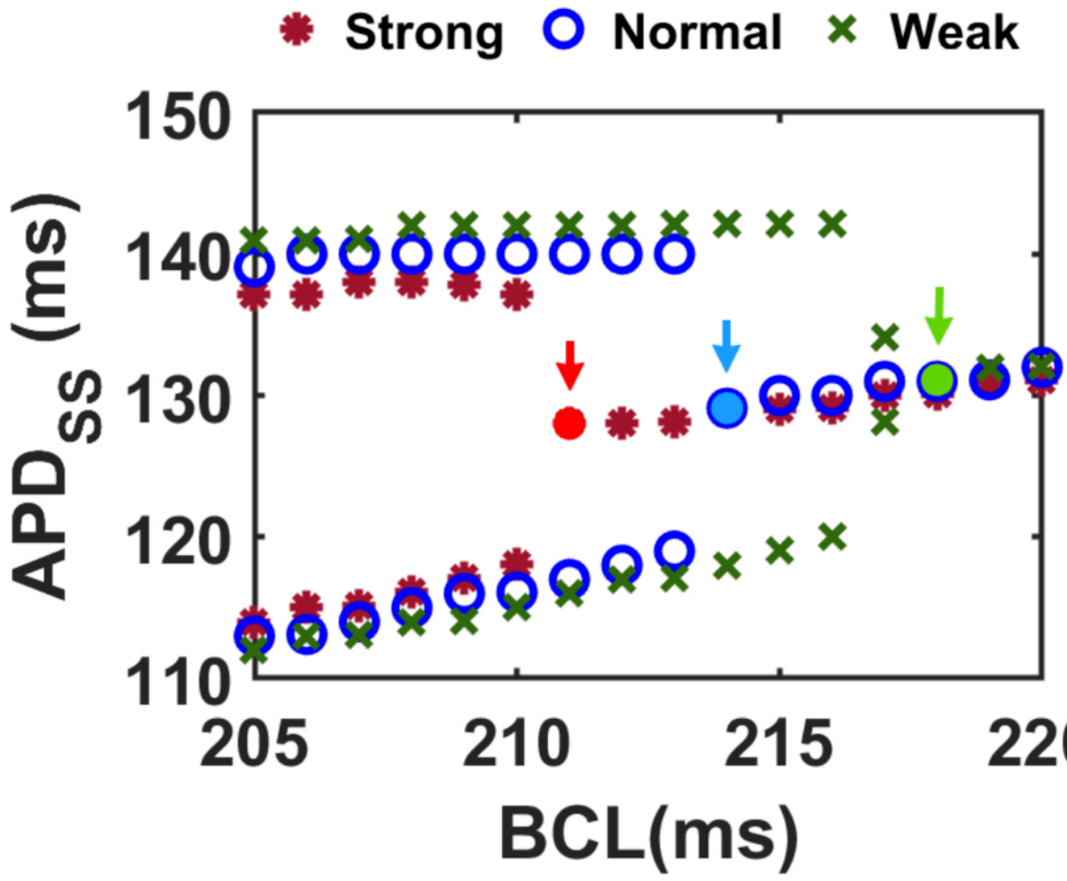

Figure 5: The effect of V-Ca coupling strength (see Table I) on the bifurcation diagram of the cardiac cell under constant-BCL pacing. The BCL_{onset} (arrows) shift to the lower values of BCL as V-Ca coupling strength increases from weak (BCL_{onset} = 218 ms) to normal (BCL_{onset} = 213.5 ms) to strong (BCL_{onset} = 211 ms) V-Ca coupling.

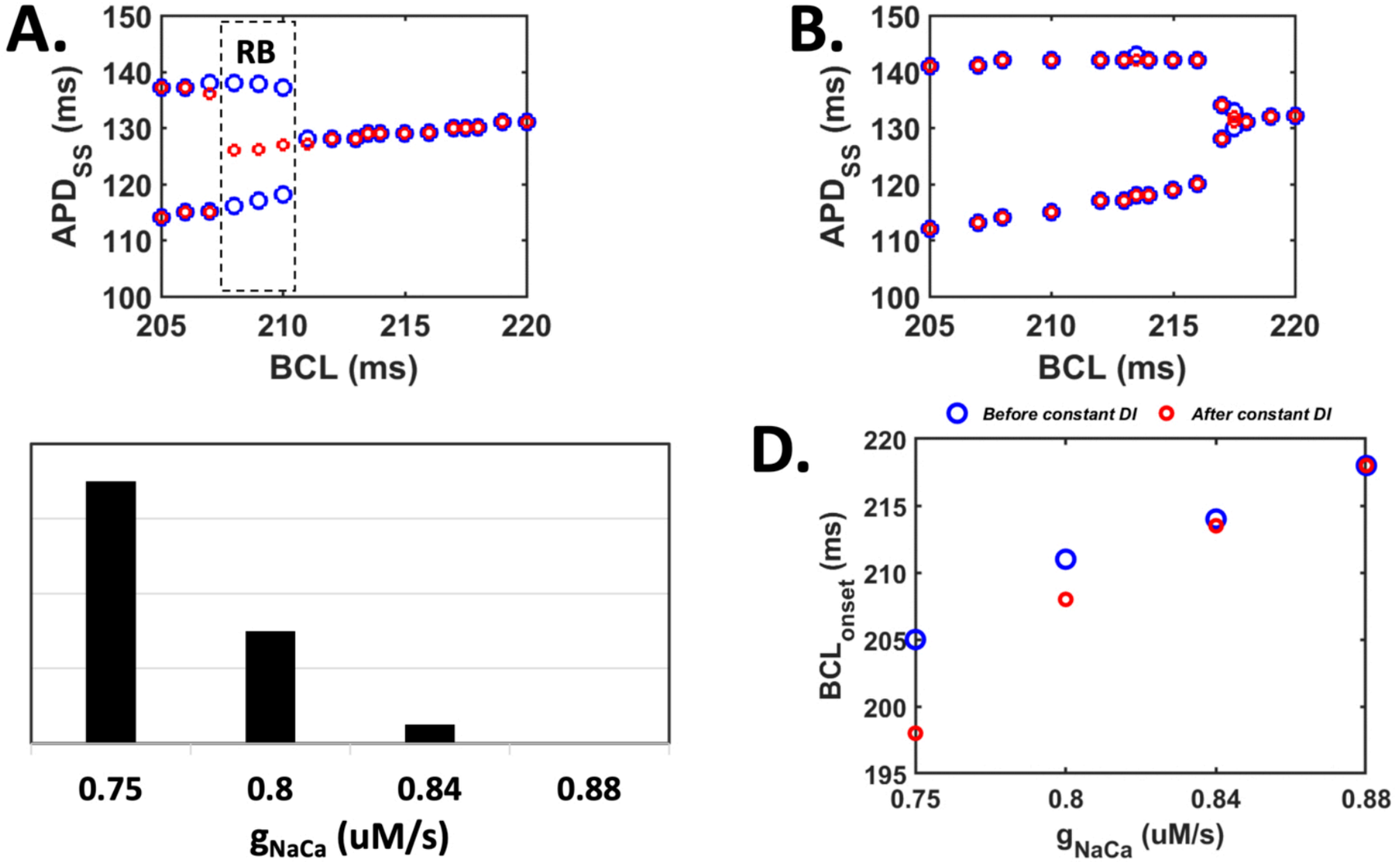

Figure 6: Overlap of bifurcation diagrams from hybrid pacing: constant-BCL pacing at BCL_1 before (blue) and after (red) constant-DI pacing for A) strong V-Ca coupling and B) weak V-Ca coupling. RB is indicated by dashed box in A. C) RB as a function of different V-Ca coupling strengths. D) The shift of BCL_{onset} before (blue) and after (red) constant-DI pacing for varying V-Ca coupling strengths.

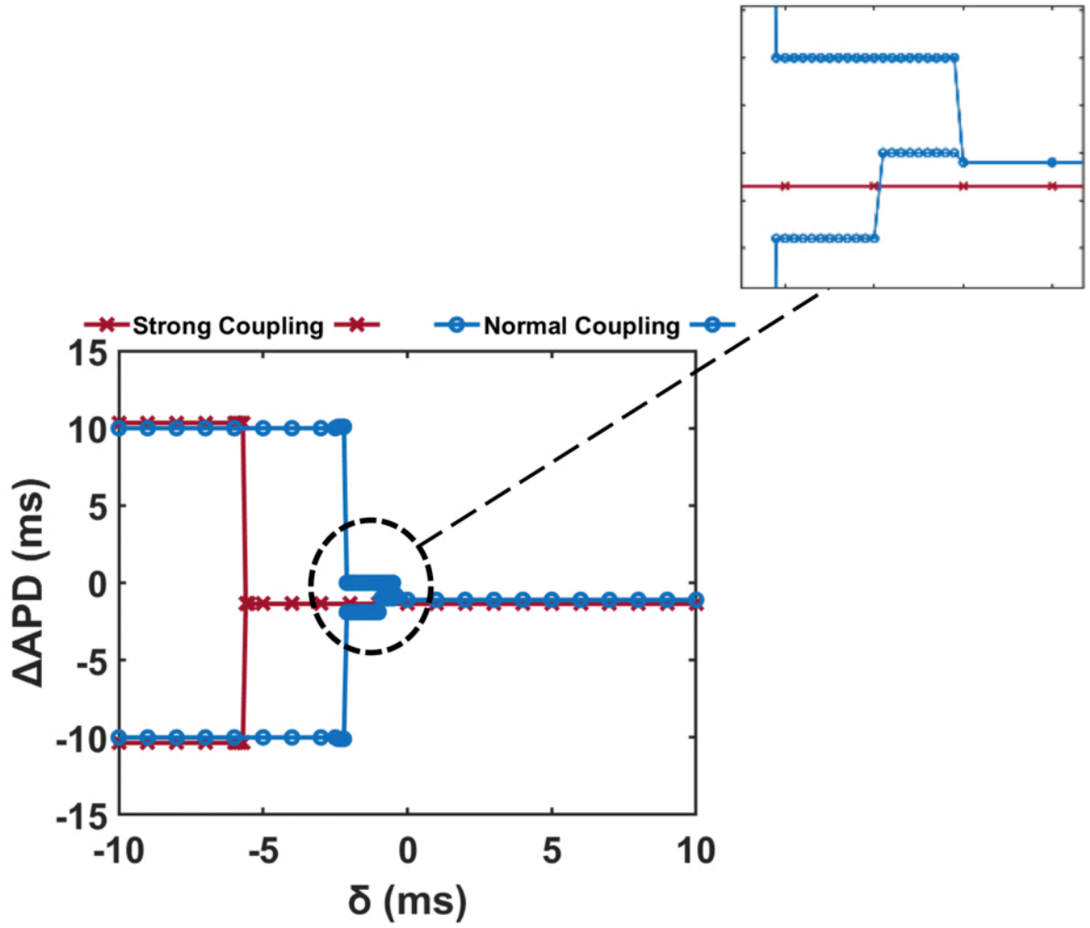

Figure 7: The magnitude of alternans ΔAPD as a function of δ when the hybrid pacing protocol with perturbation was applied for the case of strong (red) and normal (blue) V-Ca coupling.

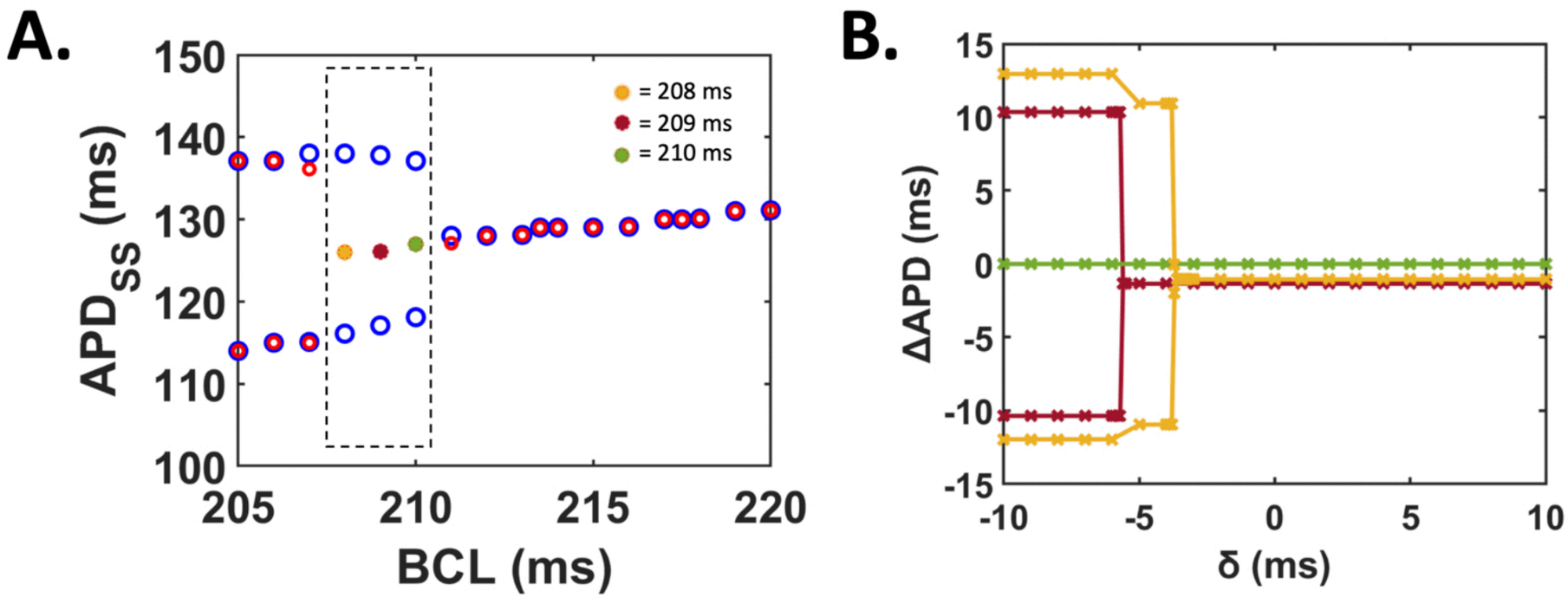

Figure 8: A) Overlap of bifurcation diagrams from three BCL_1 within RB from Fig. 6A (Table III) during hybrid pacing protocol under strong V-Ca coupling. B) The magnitude of alternans ΔAPD as a function of δ for each BCL_1 listed in Table III.